

Extreme Ultraviolet Imaging of Electron-Heated Targets in Petawatt Laser Experiments

Tammy Ma, Andrew G. MacPhee, Michael H. Key, Kramer U. Akli, Troy W. Barbee, Jr., Andrew J. Mackinnon, Richard B. Stephens, Linn D. Van Woerkom, Bingbing Zhang, and Farhat N. Beg

Abstract—The study of the transport of electrons, and the flow of energy into a solid target or dense plasma, is instrumental in the development of fast-ignition inertial confinement fusion. An extreme ultraviolet (XUV) imaging diagnostic at 256 and 68 eV provides information about heating and energy deposition within petawatt-laser-irradiated targets. The XUV images of several irradiated solid targets are presented.

Index Terms—Extreme ultraviolet (XUV) imaging, fast ignition, multilayer optics.

IN THE fast-ignition [1], [2] approach to inertial confinement fusion (ICF), a fusion target of deuterium and tritium fuel is first compressed to a high density by the use of a laser drive pulse (10 ns of ns), and then a second much shorter (~ 10 ps) high intensity laser pulse generates a high-current electron beam at the edge of the cold highly compressed plasma. The electron beam then heats a localized region to fusion temperatures, which sparks a burn wave that is able to propagate throughout the remainder of the pellet; as a result, it generates fusion energy. An advantage of this scheme as compared to conventional ICF is that the compression and heating phases are separate, which relaxes the constraints for the initial compression. However, many issues still need to be explored, including how the electrons are transported and what is the spatial distribution of energy within the target.

The interaction of an ultraintense laser with a solid target generates a large flux of energetic electrons that then heat the material, resulting in a Planckian emission spectrum extending into the extreme ultraviolet (XUV). The XUV radiation peaks as the laser energy is coupled into the target, and a hot dense plasma is created. This emission, which decreases ex-

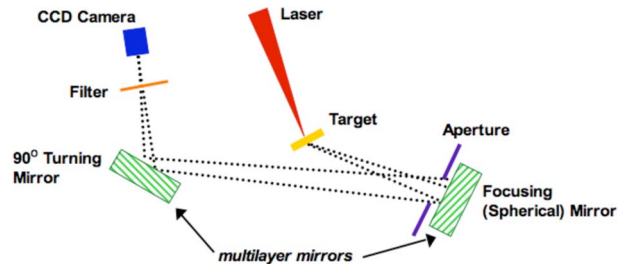


Fig. 1. Schematic of the XUV imaging diagnostic setup.

ponentially as the plasma rapidly cools, is thus short-lived [3]. Because radiation intensity varies so rapidly with temperature and the very short absorption length in the XUV, the time-integrated imaging of this radiation offers an excellent tool to measure the maximum surface temperature of dense plasma targets.

The XUV imaging diagnostic collects light within a solid angle determined by an aperture and relays this to a charge-coupled device (CCD) via two multilayer XUV mirrors that dictate the energy bandwidth. Two channels of the XUV diagnostic were employed: one optimized for 68-eV light and the other for 256-eV light. By using two different channels imaging at slightly different energies, insights can be gained about the heating, expansion, and cooling characteristics of the target (because these energies are collected from different depths within the plasma), as well as allow for the verification of thermal temperatures derived from the diagnostic. However, the temperature determinations will be discussed in a future paper, and in this article, we will concentrate on the merits of the diagnostic as qualitative imager.

The 68-eV mirrors have $\text{Mo}_2\text{C}/\text{Si}$ multilayer, whereas the 256-eV mirrors have $\text{C}/\text{WC}/\text{Monel}/\text{W}$ formula. These alternating layers of high and low indices of refraction allow for the constructive interference of X-rays to increase the overall mirror reflectivity [4]. Each XUV channel uses a pair of multilayer mirrors that are specifically manufactured to have matching spectral reflectivity. Pairing the mirrors also results in squaring the contrast against the background while additionally allowing the detector to be kept out of the straight line of hard hits. The spherical mirrors have a radius of curvature of 0.5 m, and they are placed approximately 0.27 m away from the target being imaged such that the target backside emission is reflected off the mirror. This emission is then projected onto the second multilayer (the plane mirror) at a path length of approximately 2.15 m, where it is deflected at 90° , then

Manuscript received November 30, 2007; revised March 22, 2008. This work was supported by the Lawrence Livermore National Laboratory, which is under the auspices of the U.S. Department of Energy, under Contracts DE-FG02-05ER54834, W-7405-Eng-48 DE-FC02-04ER54789 (Fusion Science Center), and DE-AC52-07NA27344. The work of T. Ma is supported by the LLNL's Institute of Laser Science and Applications Grant.

T. Ma and F. N. Beg are with the Department of Mechanical and Aerospace Engineering, University of California at San Diego, La Jolla, CA 92093 USA (e-mail: tyma@ucsd.edu).

A. G. MacPhee, M. H. Key, T. W. Barbee, Jr., and A. J. Mackinnon are with the Lawrence Livermore National Laboratory, Livermore, CA 94550 USA.

K. U. Akli and L. D. Van Woerkom are with The Ohio State University, Columbus, OH 43210 USA.

R. B. Stephens is with General Atomics, San Diego, CA 92121 USA.

B. Zhang is with the University of California at Davis, Davis, CA 95616 USA.

Digital Object Identifier 10.1109/TPS.2008.924511

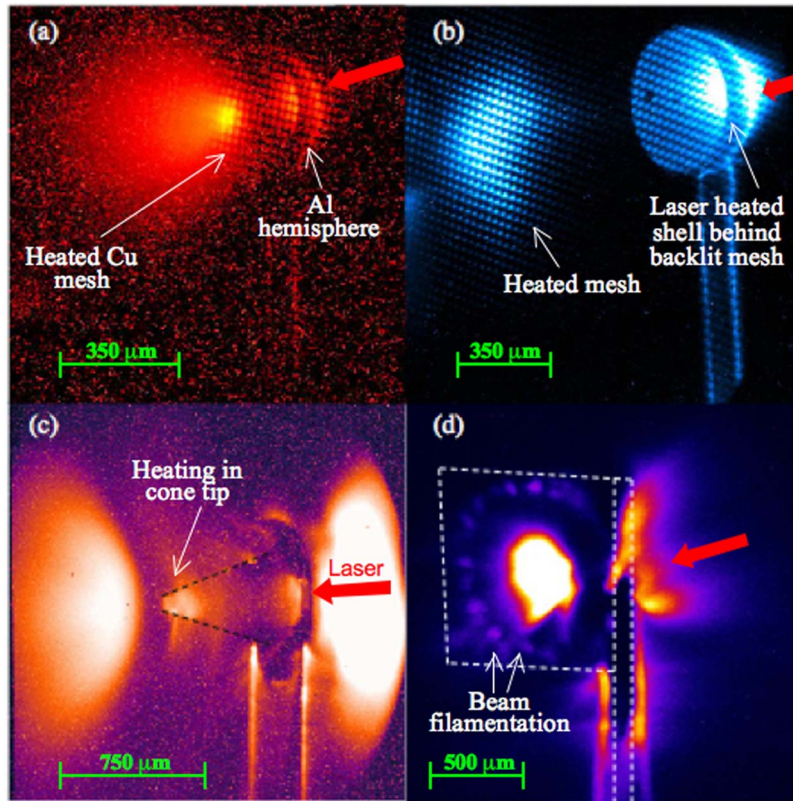


Fig. 2. (a) A 256-eV image of a half sphere with a grid $228 \mu\text{m}$ behind it. (b) A 68-eV image of a half sphere with a grid $804 \mu\text{m}$ behind it. (c) A 68-eV image of a copper cone. (d) A 68-eV image of a $10\text{-}\mu\text{m}$ CD/ $5\text{-}\mu\text{m}$ Al/ $10\text{-}\mu\text{m}$ CD sandwich.

goes through a filter before reaching the CCD (see Fig. 1). The thin aluminum and polyimide filter is designed to protect the CCD from visible and UV light. Princeton Instrument PI-SX:1300 CCD cameras record the images with a resolution of $20 \mu\text{m}$. The total magnification is approximately 11, and a 6-mm aperture in front of the spherical mirror gives a collection solid angle of 5.2×10^{-4} sr for a total spatial resolution of this XUV imaging technique of approximately $9 \mu\text{m}$.

The XUV system was used to image a variety of targets that were irradiated with the Titan laser at the Lawrence Livermore National Laboratory. The laser generates pulses of 500-fs duration with an energy of 150 J, where 15% of that energy is in a spot size of $5 \mu\text{m}$, for a total intensity on target of approximately $3 \times 10^{20} \text{ W} \cdot \text{cm}^{-2}$. The targets included metallic and plastic flat foils and copper hemispheres and cones. The XUV images of these different targets show the location of the interaction region, the varying thermal distribution of electrons based on target geometry, the spatial features of the plasma plumes, and any filamentation of the electron beams, as displayed in the four images in Fig. 2. Fig. 2(a) shows a 256-eV image of a $20\text{-}\mu\text{m}$ -thick Al hemisphere with a radius of curvature of $175 \mu\text{m}$ and a grid placed at $228 \mu\text{m}$ behind it. This image can be compared against the 68-eV image for a similar hemisphere but with a grid placed at $804 \mu\text{m}$ behind in Fig. 2(b). The grid is seen both backlit in the hatched pattern across the hemisphere and some distance away by the energetic particles which have

traversed to heat the mesh. A cone, which is irradiated head-on in Fig. 2(c), shows the expanded plasma plume in the cone open-end and the blow-off plasma from the cone tip. Also of interest is the concentration of energy in the cone tip. The XUV imager is valuable in that it can very clearly capture beam filamentation when it occurs, as in the case for Fig. 2(d), a $10\text{-}\mu\text{m}$ CD/ $5\text{-}\mu\text{m}$ Al/ $10\text{-}\mu\text{m}$ CD target. In this shot, the center spot is due to the direct heating of the target from the laser, whereas the smaller spots in the ring are electron beams that have filamented while traveling through the low-density plasma.

In conclusion, the time-integrated high spatial resolution XUV images of targets heated by a petawatt laser have been presented. The heating of these targets, and consequent plasma expansion, is captured to give a view of the deposition of energy.

REFERENCES

- [1] M. Tabak *et al.*, "Ignition and high gain with ultrapowerful lasers," *Phys. Plasmas*, vol. 1, no. 5, pp. 1626–1634, May 1994.
- [2] M. Key, "Status of and prospects for the fast ignition inertial fusion concept," *Phys. Plasmas*, vol. 14, no. 5, p. 055502, May 2007.
- [3] P. Gu *et al.*, "Measurements of electron and proton heating temperatures from extreme-ultraviolet light images at 68 eV in petawatt laser experiments," *Rev. Sci. Instrum.*, vol. 77, no. 11, pp. 113101.1–113101.6, Nov. 2006.
- [4] T. W. Barbee, Jr., "Multilayers for X-ray optics," *Opt. Eng.*, vol. 25, no. 8, pp. 898–915, 1986.